

Single-Particle Momentum Distribution at High Energies and Concept of Partition Temperature

T. T. Chou

Department of Physics, University of Georgia, Athens, Georgia 30602

and

Chen Ning Yang

Institute for Theoretical Physics, State University of New York at Stony Brook, Stony Brook, New York 11794

and

E. Yen

Department of Physics, Tsinghua University, Hsinchu, Taiwan

(Received 16 October 1984)

A concept of partition temperature is introduced in high-energy collisions. It is a natural mathematical consequence of the Darwin-Fowler method, and neither requires nor implies thermal equilibrium. A collision at a given incoming energy is described as an incoherent superposition of collisions with different partition temperatures. Angular distributions are then presented for $\sqrt{s} = 540$ GeV collisions.

PACS numbers: 13.85.Hd, 12.40.Ee

Description of model and concept of partition-temperature.—Chou and Yang¹ studied the distribution of events in the 540-GeV $\bar{p}p$ collider having forward-backward change multiplicities n_F and n_B . It was pointed out that the distribution with respect to $n = n_F + n_B$ is approximately Koba-Nielsen-Olesen (KNO) and that with respect to $Z = n_F - n_B$ is binomial. This separation of the KNO aspect and the stochastic aspect of multiparticle production processes gives conceptually a lucid and attractive picture of such collisions.

Assuming this separation to remain valid as $\bar{n} \rightarrow \infty$, it was emphasized by Chou and Yang that the distribution in the two-dimensional $(n_F/\bar{n}) - (n_B/\bar{n})$ plane would become more and more concentrated in a narrow region. For 540-GeV $\bar{p}p$ collisions this region is in the form of an “ellipse” as shown in Fig. 1(a). When \bar{n} becomes large, it becomes thinner and eventually collapses into a line segment [Fig. 1(b)]. This line segment is a collection of points, at each of which $n_F \approx n_B$ and both n_F and n_B fluctuate only to the extent of $n_F^{1/2}$ (i.e., like a stochastic distribution).

Accepting this picture for very high energies, we see that for fixed n_F , the distribution of n_B is stochastic. How then is the energy partitioned in the backward hemisphere? This is the question that we want to concentrate on in the present paper.

We shall assume that the energy partition for each hemisphere for a fixed $z = (n_F + n_B)/\bar{n}$ is also stochastic but subject to a number of conditions: (a) energy conservation, (b) leading particles effect (there may be more than one leading particle on each side), (c) d^3p/E probability for each particle, and (d) transverse-momentum (p_\perp) cutoff factor $g(p_\perp)$. In other words, the probability distribution for nonlead-

ing particles on each side will be taken as

$$\delta(\sum E_i - E_0 h) \prod_i (d^3 p_i / E_i) g(p_{\perp i}) \quad (1)$$

where $E_0 = \frac{1}{2}\sqrt{s}$, $E_0(1-h)$ = total energy of all leading particles, and $i = 1, 2, \dots$ ranges over all the particles (positive, negative, and neutral) on one side minus the leading particles. h is a parameter that describes the fraction of E_0 that fragments into particles in the central region. We surmise that (1) is very similar to part of the Monte Carlo program² of Alpgård *et al.* at least in spirit.

Now the mathematical problem (1) is well known in statistical mechanics as describing a *microcanonical en-*

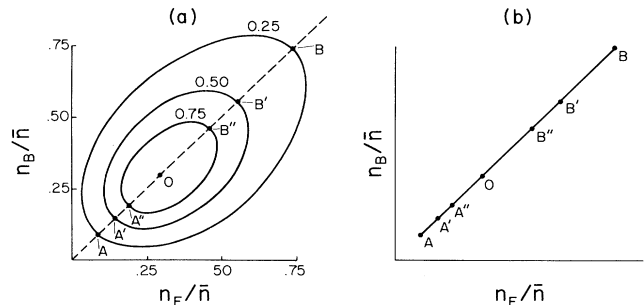


FIG. 1. Schematic diagram showing forward-backward multiplicity distribution at very high energies. (a) The contour lines represent constant values of $P(n_F, n_B) = \psi(n/\bar{n}) [2/(\pi n)]^{1/2} \exp(-Z^2/4n) = 0.25, 0.50, \text{ and } 0.75$ [see Eq. (12) of Ref. 1] at $\sqrt{s} = 540$ GeV where $\bar{n} \approx 29.1$. (b) The same contour lines degenerate to straight lines for extremely large \bar{n} . For each collision, $n_B \approx n_F$. The whole phenomenon of particle production is then an incoherent superposition of such collisions.

semble. By the well-known Darwin-Fowler method³ the single-particle distribution of such an ensemble is given by the *canonical ensemble*:

$$\text{Probability} = (d^3p/E)g(p_\perp) \exp(-E/T_p) \quad (2)$$

where T_p will be called the *partition temperature*.

540-GeV collisions.—As Fig. 1(a) shows, at the 540-GeV $\bar{p}p$ collider, the distribution is still an ellipse. We shall nevertheless test the validity of (2) at 540 GeV by evaluating the single-particle *angular distribution* from it. We write for the pseudorapidity η ,

$$\eta = \cosh^{-1}(1/\sin\theta), \quad (3)$$

$$dn/d\eta = 2\pi \sin^2\theta (dn/d\Omega) = K 2\pi \sin^2\theta \int_0^{p_{\max}} p^2 (dp/E) g(p \sin\theta) \exp(-E/T_p), \quad (4)$$

where K is a normalization constant, $p_{\max} = E_0 h$, and

$$g(p \sin\theta) = \exp(-\alpha p \sin\theta). \quad (5)$$

We take α to be equal to

$$\alpha = 2[\langle p_\perp \rangle]^{-1} = 5.25 \text{ (GeV/c)}^{-1}. \quad (6)$$

Only pions are included in this calculation. See remark (h) below. The angular distribution is evaluated from (4) and compared with the results⁴ reported by Rushbrooke. It is found that the curve for each multiplicity n is well fitted by (4) for one value of T_p . Figure 2 and Table I summarize these calculations. We emphasize that there are no adjustable parameters in this computation, the cutoff α in (6) having been taken from experiments⁷ concerning p_\perp distributions. The parameter h and normalization constant K are both determined from the curves themselves. If one takes a Gaussian p_\perp distribution instead of (5), the fit to the angular distribution is also good.

We conclude that the angular distribution (4) that results from (2) is in excellent agreement with experiment. It seems that (2) would give a complete description of the single-particle momentum distribution for nonleading particles. *It is, however, important to experimentally test the two-dimensional distribution of (2) directly by, for example, measuring the single-particle momentum distribution at fixed angles.*

Remarks.—(a) The partition temperature T_p is a parameter that controls the energy partition on one side of the collision. *No thermal equilibrium is implied.* This is a very different concept from the temperature idea for high-energy collisions used in previous theories.⁸

For a collision with a large impact parameter (Fig. 3), the two shaded regions do not have much chance of exchanging longitudinal momenta. Therefore, these two areas tend to maintain their respective original velocities in the center-of-mass system. One thus expects the average energy per particle that results from these to be large. That is, T_p should be large. On the other hand, for small impact parameters b , the two shaded regions of Fig. 3 are expected to exchange a lot of longitudinal momenta, resulting in smaller average energy per particle emitted and therefore smaller T_p . This qualitative expectation is borne out by Table I.

(b) The parameter h is related to the “inelasticity” used in cosmic-ray physics.⁹ Its definition has always involved great uncertainties conceptually, because for small θ (large η) a single emitted particle can contribute a very large energy and it is not clear whether one should consider such particles as leading or not. With the concept of T_p , which is numerically determined from the bulk of the lower η data, the parameter h can be more accurately determined from (2) by integration.

(c) The angular distribution in Fig. 2 exhibits a high- η cutoff and a valley at $\eta = 0$. These characteristics can be understood as follows. If we put the emit-

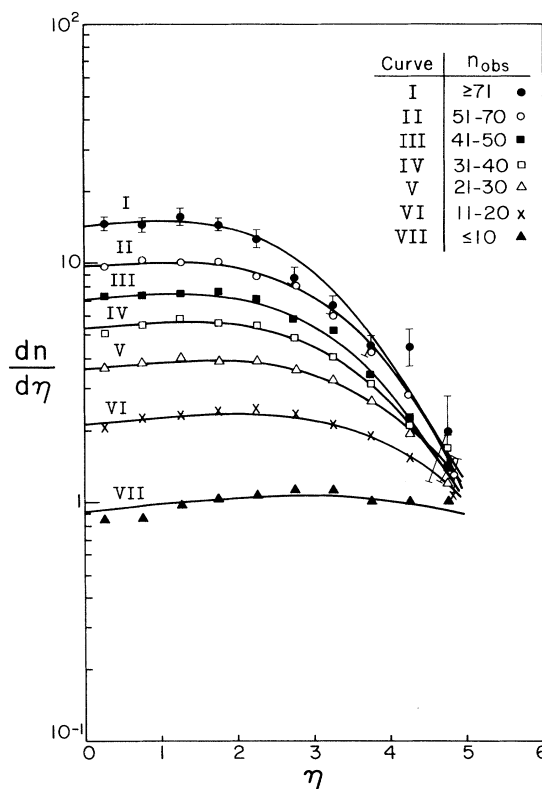


FIG. 2. $dn/d\eta$ vs η at $\sqrt{s} = 540$ GeV. Curves are calculated from Eqs. (4)–(6). Data points are taken from Ref. 4.

TABLE I. Parameters for inelastic collisions. n_{obs} which labels different multiplicity ranges is different from the true multiplicity by a factor of approximately 1.25 due to experimental corrections (see Ref. 5). The average values of the impact parameter are rough estimates based on Fig. 1 of Ref. 6.

n_{obs}	Partition temp. T_p (GeV)	Av. energy per particle in central region (GeV)	Energy fraction in central region, h	KNO variable $z = n_{\text{cal}}/\bar{n}$	Av. impact parameter $b(F)$ (approx.)	Norm. constant K (GeV) $^{-2}$	n_{cal}
≥ 71	4.38	1.64	0.451	3.42	< 0.05	82.9	99.4
51-70	6.25	2.06	0.419	2.52	0.1	54.0	73.3
41-50	6.80	2.17	0.332	1.89	0.3	39.5	55.0
31-40	8.84	2.57	0.316	1.52	0.5	29.3	44.2
21-30	13.8	3.35	0.308	1.14	0.8	19.5	33.0
11-20	23.8	4.36	0.257	0.73	1.2	11.2	21.2
≤ 10	183	6.63	0.197	0.37	1.7	4.76	10.7

ted particle's mass (m_π in our computation) to zero, then the angular distribution becomes

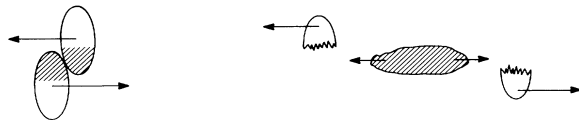
$$dn/d\eta = 2\pi K (\alpha + T_p^{-1} \cosh\eta)^{-2}. \quad (7)$$

This exhibits clearly the high- η cutoff which originates from the $\exp(-E/T_p)$ factor in (2). The valley at $\eta=0$ is a consequence of the fact that the integrand in (4) decreases with increasing θ . Furthermore (7) also shows that if $m_\pi=0$, the $dn/d\eta$ versus η curve is monotonically decreasing with increasing η , exhibiting no valley at $\eta=0$. That is, the valley is absent if $m_\pi=0$. It follows that the valley would deepen if one takes into account the production of higher-mass particles such as the kaon.

(d) Because the distribution in Fig. 1(a) is not yet a thin ellipse at 540 GeV, both T_p and h should not be expected to assume single values at a fixed $z = n/\bar{n}$. But in Fig. 2 and Table I we ignore this fluctuation of T_p and h .

(e) The Bloch-Nordsieck factor $1/E$ in d^3p/E is essential. If one deletes this factor from the integrand in (4), the angular distribution is drastically changed and would not resemble the experimental curves at all.

(f) In the model described above, illustrated in Fig.



BEFORE COLLISION

AFTER COLLISION

FIG. 3. Schematic diagram for high-energy inelastic collisions. The incoming hadrons are represented as extended balls of quark-gluon matter, Lorentz-contracted. Their unobstructed parts sail through to form leading particles. The central region are emitted from the overlap (shaded) region.

3, for very high energies there is a parameter h_F for each collision which represents the fraction of the incoming forward hadron energy that fragments into central region particles. There is also a similar h_B which is $\simeq h_F$. Notice the strong correlation between h_B and h_F . There does not seem to exist experimental information about this correlation. What has been studied is a quantity x_F^{lead} for the leading forward proton defined by Basile *et al.*¹⁰ It is related to h_F by

$$x_F^{\text{lead}} + h_F < 1, \quad (8)$$

because there may be other leading particles beyond the leading proton. Only when there are no other leading particles, would the unequal sign in (8) be replaced by an equal sign.

(g) We have shown above that expression (2) gives a good description of the single-particle spectrum. While this expression was derived from (1), it does not follow necessarily that (1) gives a good description of the exclusive spectrum. In particular (1) implies that the two-particle correlation for $+$ - particles is the same as that for $+$ + particles, a conclusion that may or may not be correct at $\sqrt{s} \geq 540$ GeV. *It seems to us that this is an important question to be studied experimentally.* Such study would resolve the question of whether a cluster model¹¹ or the model described by (1) above gives a better description of the two-particle inclusive spectrum. (Both give a good description of forward-backward asymmetry.¹)

While (1) may or may not be modified because of correlation studies, we emphasize that the *concept of partition temperature T_p will remain after any such modifications*: The concept of T_p originates in (i) the δ function in (1) representing energy conservation, and (ii) the Darwin-Fowler method of steepest descent. Both clearly will survive any modifications of (1), and $\exp(-E/T_p)$ will always be one of the factors of the single-particle distribution for the nonleading particles.

(h) It is known⁷ that the K/π ratio increases with increasing energy. For any accurate fit with experiments, the kaons will have to be included.

(i) We have made extrapolations of the angular distribution to higher energies. The results will be published elsewhere. Also discussed there will be the relation between the ideas in the present paper and those in earlier works on cosmic rays and high-energy physics.

This work is supported in part by the U. S. Department of Energy under Grant No. DE-FG09-84ER40160, and by the National Science Foundation under Grant No. PHY 81-09110 A01.

¹T. T. Chou and Chen Ning Yang, Phys. Lett. **135B**, 175 (1984).

²K. Alpgård *et al.*, Phys. Lett. **107B**, 310 (1981).

³C. G. Darwin and R. H. Fowler, Proc. Cambridge Philos. Soc. **21**, 730 (1923), and earlier papers.

⁴J. G. Rushbrooke, in *Proceedings of the Fourteenth Inter-*

national Symposium on Multiparticle Dynamics, Lake Tahoe, 1983, edited by J. F. Gunion and P. M. Yoger (World Scientific, Singapore, 1984).

⁵UA5 Collaboration, presented by D. R. Ward, in *Proceedings of the Third Topical Workshop on Proton-Antiproton Collider Physics, Rome, 1983*, edited by C. Bacci and G. Salvini (CERN, Geneva, 1983).

⁶T. T. Chou and Chen Ning Yang, Phys. Lett. **116B**, 301 (1982).

⁷J. G. Rushbrooke, in Proceedings of the DPF Workshop on $\bar{p}p$ Options for the Supercollider, Chicago, February 1984 (to be published).

⁸E. Fermi, Prog. Theor. Phys. **5**, 570 (1950); S. Z. Belen'kji and L. D. Landau, Nuovo Cimento Suppl. **3**, 15 (1956); R. Hagedorn, Nuovo Cimento Suppl. **3**, 147 (1965). The partition-temperature concept seems to be also different from the essence of the model of Chou Kuang-chao, Liu Lian-sou, and Meng Ta-chung, Phys. Rev. D **28**, 1080 (1983).

⁹G. Cocconi, Phys. Rev. **111**, 1699 (1958). See also Ref. 6.

¹⁰M. Basile *et al.*, Nuovo Cimento **73A**, 329 (1983). Compare also with the theory of J. Benecke, A. Bialas, and S. Pokorski, Nucl. Phys. **B110**, 488 (1976).¹

¹¹K. Alpgård *et al.*, Phys. Lett. **123B**, 361 (1983).